Stochastic Modelling and Computational Sciences

CONSOLIDATION OF SQUEEZE AND EXCITATION WITH VGG16 FOR PNEUMONIA DIAGNOSIS THROUGH CHEST X-RAY IMAGES

Kanchan Dabre[*1], Satishkumar L. Varma[2] and Pankaj B. Patil[3]
[1]Department of Computer Science and Engineering (Data Science), D. J. Sanghvi College of Engg, Mumbai, India
[2]Department of Information Technology, Pillai College of Engineering, New Panvel, India
[3]Consultant Radiologist and Sonologist Doctor, Cardinal Gracious Hospital, Vasai, Sunlab Diagnostics Ltd., Virar, India
[1]kanchandabre@gmail.com
[1]ORCID ID: 0000-0003-4246-9395

ABSTRACT
Pneumonia is a life-threatening thoracic disease caused by a bacterial infection in the lungs. A chest radiography is a common diagnostic test to perceive pneumonia. Generally, radiologists or skilled medical professionals locate and identify pneumonia clouds in CXR. Modern computer aided pneumonia diagnostic techniques uses deep learning architecture which allocates equal weightage to all extracted feature maps calculated after applying stacking of convolutional and pooling layer for the final result prediction. This mechanism is not effective as few feature maps can be redundant or irrelevant and may not contribute effectively in pneumonia classification. Hence in this research squeeze and excitation network is used over VGG16 base model's extracted feature maps to calibrate them by assigning the appropriate weights based on its effectiveness in pneumonia disease prediction. The suitable preprocessing and augmentation techniques are selected before extracting the global and local statistical object detection features through careful enhancement in both architecture and training strategies. This deep model's effectiveness and robustness are examined, and its performance is quantitatively assessed by comparison with cutting-edge methods like vanilla VGG16, EfficientNetB7, MobileNetV2, XceptionNet with freezing and unfreezing VGG16 base layers using pertinent evaluation metrics over readily available baseline datasets for kermany pneumonia. The squeeze and excitation integration with VGG16 architecture exhibited a high accuracy of 96.69% in classifying pneumonia from thoracic images. Radiologist, Sun Lab Diagnostic, Virar, and Cardinal Gracious Memorial Hospital, Vasai, assist the clinical execution and validation of this research findings.

Keywords: deep learning, pneumonia, CXR, chest X-Ray diagnosis, Squeeze and Excitation (SE), convolutional neural network

1. INTRODUCTION
A frequent respiratory infection affecting both adults and children is pneumonia [1]. It is triggered by bacteria or viruses and attacks small balloon-shaped sacs at bronchioles ending in the pulmonary alveoli. Lung opacities, which appear more opaque on CXR, indicate that the lung tissue is likely not healthy [5]. Pneumonia is the most common cause of mortality and morbidity worldwide [21] [37] [53]. Figure 1 shows healthy and pneumonia infectious lung images.

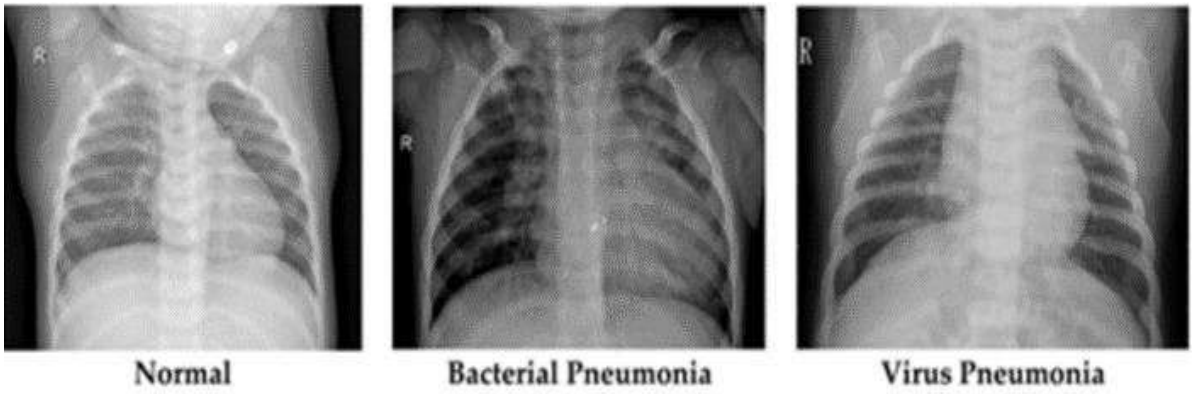

Fig. 1: Type of pneumonia diseases [27]

Pneumonia disease diagnosis is possible through different medical screening such as lung ultrasound [11] [14], computerized tomography (CT) [39] [51], volume sweep imaging [46] [47], magnetic resonance imaging (MRI) [49-50] and Chest X-Rays (CXR) are one of many possible medical imaging modalities used in screens for the diagnosis of pneumonia. Due to its quick imaging time, minimal radiation exposure, and low cost, chest X-rays are a prominent imaging modality in the diagnosis of thoracic anomalies in clinical settings [11-12]. There are challenges in computer aided pneumonia diagnostic [14] such as the imbalanced dataset, limited quality of chest radiograph processing, overlapped patterns of opacities, presence of strong edges at the clavicle rib cage, too small costophrenic angle different types of feature statistics used for segmentation and identification [22] [28].

Accurate disease prediction requires suitable annotated, preprocessed, augmented, normalized images for segmentation [28] [34] and classification. An efficient second opinion providing assistive methodology is much needed for precise detection of pulmonary pneumonia infection through careful enhancement in both architecture and training strategies using deep learning. This study can help in standardization in patients' care through timely diagnosis, reducing human biased error, as well as enhancing the current computer aided diagnostic system.

2. LITERATURE SURVEY

Machine learning models [44] [52] [54] detect pneumonia and non-pneumonia patients using CXR images, with deep learning techniques [18] [20] [25] [[32] improving classification accuracy by changing convolutional layers and transfer learning for pneumonia diagnosis.

Jianpeng Zhang suggested CAAD- confidence aware anomaly discovery model, which includes a shared pattern extractor, an anomaly discovery module for detecting anomaly i.e. viral pneumonia which was major cause of COVID-19 attains a sensitivity of 71.70 percent and an AUC of 83.61 percent. The degree of abnormalities in a specific image is described by a confidence prediction network ranging from very proven positive to verified negative cases.

Amal H. Alharbi et. al. [55] proposed two Box-ENet prototypes and pretrained models are compared for pneumonia recognition from segmented X-rays. Results show segmented pulmonary X-ray classification is more reliable with 97.40% accuracy. Tatiana Gabruseva proposal a simple, effective algorithm for localizing lung opacities using RetinaNet, Se-ResNext101 encoders, and ImageNet dataset, achieving optimal threshold for the NMS- non-maximum suppression algorithm achieved 0.23908 mAP on the private custom test dataset [56].

The ensemble method trained seven CNN (Xception, ResNet-50, Inception-V3, VGG-16, VGG-19, MobileNet, and SqueezeNet) models on the ImageNet dataset, with the ensemble approach was chosen for three effective models. The technique had a fantastic AUC of 95.21 and sensitivity of 97.76. , and multi class classification accuracy of 90.71 in chest X-ray images suggested by Ayan et. al. [57].

Table 1 shows literature survey of existing pneumonia diagnostic method using image processing based feature

analysis with and without segmentation [42] [48], machine learning based feature extraction with and without segmentation techniques, Deep learning and transfer learning techniques with and without segmentation [36] [41] [43]. Table highlights dataset used with count of radiological images, evaluation parameters to analyse the classification performance, obtained results and the associated scope for further studies and expansion. Different method has its own limitations and advantage it is clearly seen that over the evolution of deep learning and machine learning techniques the prediction results have got improved.

3. PROPOSED ARCHITECTURE

The general architecture of Chest X-Ray interpretation is through the following stages shown in Figure 2, where data collection, image pre-processing, data augmentation, pretrained model image embedding extraction, attention mechanism, encoded features and disease classification based on observations made and conclusions are drawn.

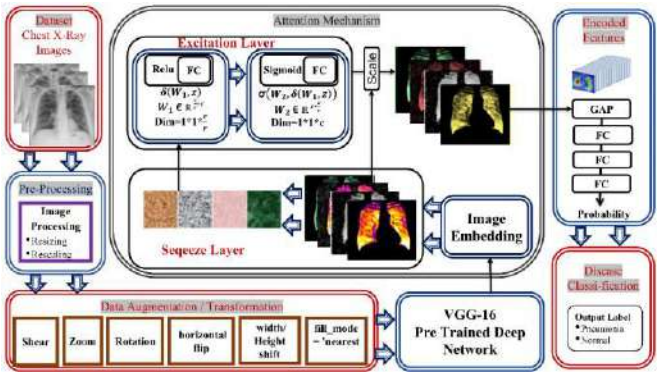

Fig. 2: Deep architecture in detection of pneumonia disease using Chest X-Ray images

Over the advancement in machine and deep learning techniques, the main phases of feature learning and disease prediction gets replaced by deep neural networks like convolutional neural network architecture takes a chest radiogram as input and extracts its meaningful features which are then weigh it based on squeeze and excitation block.

3.1. Dataset

Kaggle CXR pneumonia images dataset, is a licensed standard publicly available dataset for disease classification. Dataset comprises 5,863 CXR images in JPEG format under 2 categories. The pneumonia chest X-ray represents regions of aberrant opacification in the lungs and healthy chest X-Ray indicates clear lung in the image. Pneumonia X-Ray images are further divided into Viral pneumonia displays a more widespread "interstitial" pattern in both lungs than bacterial pneumonia, which shows localized lobar consolidation.

At Guangzhou Women and Children's Medical Center, a posterior and anterior CXR images were collected over a period of time from cohorts of pediatric patients between the age group of one and five years. These chest X-ray images were removed as part of the regular clinical care for the patients. These collected chest x-ray images were analyzed before adding to the dataset. All unreadable or poor quality scans were removed during initial screening of chest radiograph for quality control. In the last phase, annotation and grading of diagnoses was performed on every radiograph by three experienced medical professionals before approval for training over AI systems. [40]. Ground truth labeling is done with the help of radiologists. Figure 10 highlights pneumonia dataset split based on training and testing samples distribution.

3.2. Preprocessing

Second stage of computer aided diagnosis is preprocessing publically available standard chest X-Ray datasets [3] [8]. Standard image preprocessing techniques viz. contrast enhancement, resizing and rescaling is applied to chest radiography. All chest X-Ray to produce a uniform quantification, collected photos are solely cropped. To provide the necessary input for deep architectures, all photos are scaled to 150*150 square pixels. Every single input image given to the encoder models will undergo these preprocessing operations. during training and

evaluation phases. The input dataset is divided into three portions for testing, training, and validation: 85:10:5. Preprocessing and normalization of images are vital for accurate disease detection. Following Augmentation techniques are followed in pneumonia disease diagnosis using X-Ray.

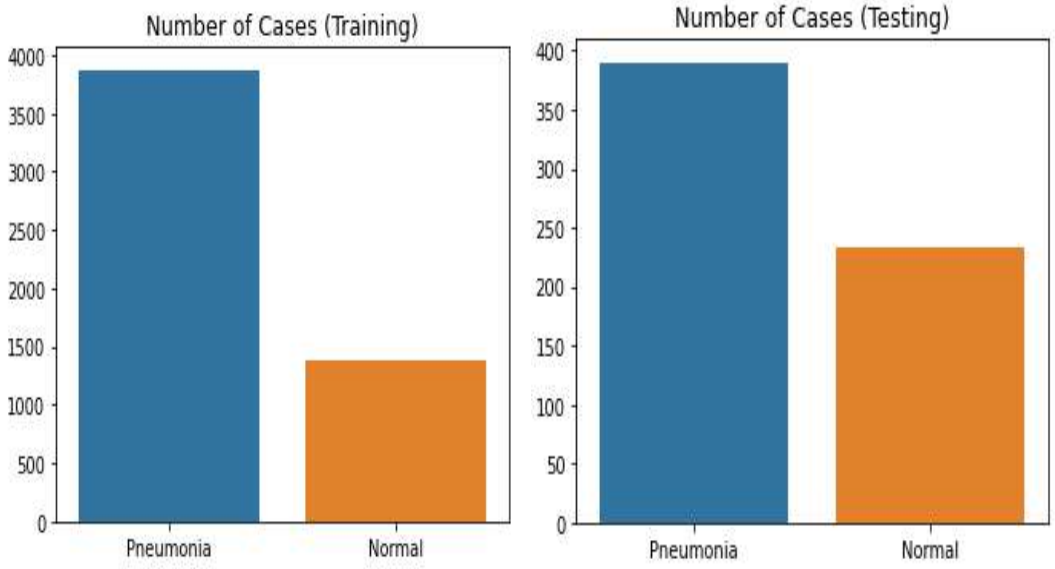

Fig. 3: Analysis of dataset split for training and testing

All chest X-Ray to produce a uniform quantification, collected photos are solely cropped. To provide the necessary input for deep architectures, all photos are scaled to 150*150 square pixels. Every single input image given to the encoder models will undergo these preprocessing operations. during training and evaluation phases.

Table 1: Literature review of deep networks used for pneumonia disease detection.

Techniques	Study	Methodology	Datasets/ #images	Results of Datasets Assessment measures	Research Gap
Image Progressing Based Pneumonia Disease Feature Detection	Armato et al., 1998	Iterative global thresholding, Smoothing Method	Custom/ 600	Subjective evaluation of accuracy Up to 79.1%	Need priori knowledge about overall lung morphology, Lack of Robustness to Noise and Variations.
	Li et al., 2001	Iterative contour-smoothing algorithm, pattern categorization, and image feature analysis	Custom/ 40	91% sensitivity 95.2% accuracy 96.5% specificity;	False boundary points located on medial and diaphragm edges
	Iakovidis et al. , 2008	Salient control points for bezier interpolation	Custom/ 24	94.3% specificity, 95.3% sensitivity	Shape prior information was not considered, Not able to

					adapt to changes
	Van Ginneken et al. 2016	SMOTE (Synthetic Minority Over-sampling Technique)	Custom/ 230	Right lung: 0.929± 0.026 Left lung: 0.887 ± 0.114	Lower sensitivity, missed context features extracted from patches
Image processing with lung segmentation	Cheng et al. 1988	Grey level histogram thresholding,	Custom	Accuracy Up to 72%	Existence of extraneous regions on both sides of the lungs
	Van Gin neken et al.,2006	Pixel classification algorithms, deformable models, rule-based and hybrid techniques.	Custom/ (230)	Overlap scores right lung:0.929 ± 0.026 Left lung: 0.887 ± 0.114;	limitations of manual segmentations, difficulty in identifying fundamental differences between pixel
	Wang et al, 2015 [17]	Oriented Gaussian derivatives filter. Fuzzy C-Means (FCM) clustering and thresholding	JSRT Custom/ (154)	Accuracy, precision >90% over lap score=87%	Single slice of CT images considered to measure the liver volume, lung field is not properly segmented on mobile radiography
Machine Learning Methods	Mcnittgray et al. ,2001	Active Appearance Model	Custom/ 33	Accuracy : LDA:70%, KNN:70%, NN: 76%;	Cannot be used for topology variation
	Vittitoe et al. ,1998	Markov random field modeling	Custom/ 198	Specificity: 0.972 ± 0.022; Sensitivity: 0.907 ± 0.044	Relatively slow convergence time 150 sec, atypical situations were not covered such as gassy stomachs and large lung regions, small size clique sets
	Shi et al.,2009	Gaussian Kernel-based FCM	JSRT/ 52	Accuracy: 0.978	Results were preliminary without

					validation
	Novikov et al. ,2017 [35]	Fully convolutional architectures	JSRT/ 52	Jaccard coefficient, : 97.4%, Dice coefficient: 95%;	Difficult to determine which additional deep NN branches benefits and which adds complexity
	Dai et al., 2017[7]	Structure Correcting Adversarial Network	JSRT, MC	IoU: 94:7% ± 0:4%, heart:	Lung field with alike intensity and texture as outer boundary, leading convolution to fail in middle two column
	Tej et.al., Springer con, 2018 [33]	Multilayer Perceptron, Random Forest, Logistic Regression	NIH ChestXray14 dataset	Acc: 95.63, Recall: 93.68, Precision: 97.57	Missing statistical feature of the lungs airspace
Table 1. Continued					
Techniques	**Study**	**Methodology**	**Datasets/ #images**	**Results of Datasets Assessment measures**	**Research Gap**
Deep learning networks	Jaiswal et. al. Meas. J. Elsevier, 2019. [13]	Mask R-CNN	RSNA pneumonia dataset	MTV:0.098189, MS:0.100155	Obtained weaker results on the training set with respect to the test while reducing overfitting
	Okeke et al, J. Health care Engg, 2019 [30]	DenseNet 512	Pediatric dataset	Train Acc:0.9531 Val Acc:0.9373	demands enormous time, know-how, and resources
	T. Rahman et al MDPI, App Sci, 2020 [27]	AlexNet, ResNet18, DenseNet201, SqueezeNet	ChestX-ray14 PLCO dataset	Recall: 99.0, Precision: 97.0, AUC: 98.0, Acc: 98.0	Large degree of variability in the input images reduced performance
	V. Chouhan et al, App Sci, oct 2020 [4]	AlexNet, DenseNet121, InceptionV3, resNet18, GoogLeNet	Kermany dataset	Accuracy:96.4% Recall: 99.62%	Missing semantic segmentation with

					explanations, overfitting
	Khalid et.al, arxiv, 2020 [7]	Resnet50	Chest X-Ray, CT dataset	Acc: 96.27, Recall: 94.92 F1 Score: 96.67	Lack of biomedical image segmentation
	Togacar et.al, Elsevier, IRBM, 2019 [31]	AlexNet, VGG-16 and VGG-19(ML augmentation)	Pneumonia dataset	Acc: 9.41, Recall:99.61, Precision:99.22, F1Score:99.41	Need of robust and consistent deep features
	Tatiana et.al. IEEE, CVF, 2020 [8]	RetinaNet SE-ResNext 101	US National Institutes Health Clinical Center	IoU: 0.25	Lazy Stable and robust model to detect occurrence of fuzzy white clouds in the lungs
Deep Learning with Lung Segmentation Prediction	Pranav Rajpurkar et al, 2017 [8]	ChestNet	ChestX-ray14 PLCO dataset	AUC:0.74 to 0.78	Missing learning the correlations among disease image
	Khalid et. Al, 2020 [19]	DenseNet	ChestX-ray14 (2017) MIMIC-CXR	AUC:0.81 to 0.82.	Minor outliers and feature overlap between normal and pneumonia
	Yuan Xue et al, summers, 2019	Tie-Net[9]	OpenI ChestX-ray14 Hand-labeled	AUC:.87 to .96 METEOR 0.10 ROUGE-L 0.22	Absence of multiple RNNs for feature attribute with correlation
	Arun Prakash et. al., Multimedia, 2022	DenseNet121[10]	Hospital of China Medical University	Accuracy 0.87 precision 0.73 F1 Score 0.66	Exclusion of questionable reports
	Jianpeng Zhang et al, IEEE Trans. 2020 [45]	InvertedNet[2]	JSRT dataset [6]	Accuracy 0.87, AUC 0.87, F1Score 0.66, precision 0.73	Loses information about specific locations trade-off between depth and computational feasibility
Areas Under Curve (AUC), Intersection over-union (IoU) Mean average precision (mAP), Mean threshold value(MTV), Mean score(MS)					

The input dataset is divided into three portions for testing, training, and validation: 85:10:5. Preprocessing and normalization of images are vital for accurate disease detection. Following Augmentation techniques are followed in pneumonia disease diagnosis using X-Ray.

3.3. AUGMENTATION

Augmentation is a process of exaggeratedly growing the diversity of training data to enhance the performance and robustness of models trained on image data. The model generalizes better to different scenarios and increase its capacity to manage variations in the input data by transforming the original radiograph in numerous ways.

Rotation: Rotating images by 300 angle to create new training examples to recognize objects or patterns in images, regardless of their orientation.

Rescale: This scaling transformation involves resizing images by 1/255 factor as there are 256 gray levels present in original X-Ray image, to handle variations in object sizes and improve its performance on images with different scales.

Shear Transformation: Shearing refers to a transformation that skews the image along one axis while keeping the other axis unchanged. In shear range augmentation, a shear transformation is applied within a specified range of 10 angles to create augmented versions of the CXR image.

Zoom: Zoom augmentation is especially useful for training models to handle varying objects' distances from the camera or to improve their capacity to identify objects at different scales of 0.2 by welcoming deviations in object sizes and spatial relationships within the images.

Horizontal flip augmentation: Horizontal flip augmentation helps models become more invariant to left-right orientation. As CXR are taken from front as well as from back scan both are used for screening pneumonia.

Width/Height Shift: This technique involves shifting the pixels of an image along the width and/or height dimensions in 0.2 range to become more robust to changes in lung position within the image and enhances their ability to handle variations in object location.

Fill Mode: This mode involves using the pixel value from the nearest non-empty pixel in the original image to fill the empty area. It helps maintain the original pixel values as much as possible while performing operations such as rotation, scaling, shifting, and other transformations that might leave parts of the image empty or uncovered.

3.4. TRANSFER LEARNING

Transfer learning leverages the acquaintance and educated features from a pre-trained model resulting in faster training and improved performance. Pretrained models usually consist of a feature extraction part i.e. bottom layers and a task-specific part i.e. top layers. VGG16 architecture which was built on objective of recognizing object shapes has excellent layerwise feature extraction vision mechanism. VGG16 is used in this research as a base model and been modified with replacing the top layers. These top layers are responsible for the final pneumonia-specific predictions. In this research, evaluation of model performance on pneumonia prediction is been conducted by freezing and releasing the weights of the base feature extraction layers during initial training. This means these layers will retain the learned features from the original task and won't be updated during training on the pneumonia prediction if freezes. This helps preserve the valuable features learned from the larger dataset. In deep neural network layers when there are different feature maps having different features extracted, it is quite obvious that few feature maps might be redundant or irrelevant which may not contribute effectively in pneumonia classification. Hence squeeze and excitation network is introduced in between layers which calibrates channels and assigns the appropriate weights to extracted feature maps based on its effectiveness in pneumonia disease prediction. Experimentation and understanding the nuances of the models and tasks are crucial for effective transfer learning.

3.5. Consolidation of Squeeze And Excitation (SE):

SE- Squeeze and Excitation is a method for modelling channel interdependencies in convolutional neural networks (CNNs), enhancing their representational capability. It focuses on channel-wise feature recalibration, highlighting crucial channels while suppressing less valuable channel. The SE block consists of excitation and squeeze, with the squeeze procedure reducing input feature maps to a single channel. Global average pooling collects information about global locations, and the channel descriptor represents its relevance. For each channel c in the feature map:

Squeeze Operation: Compute the global average pooling (GAP) across spatial dimensions (height and width) for each channel to obtain a channel-wise statistic as shown in Equation 1.

$$z_c = \frac{1}{H.W} \sum_{i=1}^{H} \sum_{j=1}^{W} x_{i,j,c} \quad (1)$$

z_c is the output value for channel c after global average pooling. The feature map's height is denoted by H. The feature map's width is denoted by W. $x_{i,j,c}$ represents the value of the pixel at position (i, j) in channel c of the feature map. FC layers identify connections and calculate channel-specific weighting coefficients, and input feature maps are given recalibration weights by multiplying each channel by the corresponding weight. This process enhances the network's discriminative power and performance in pneumonia classification.

Excitation Operation: Transform the channel-wise statistic zc using two fully connected (FC) and non-linear activation function layers i.e. ReLU as shown in Equation 2.

$$S_c = \sigma(W_1 . z_c + b_1) \quad (2)$$

S_c is the output of the first FC layer for channel c. W_1 and b_1 are the weights and bias of the first FC layer, respectively. σ is the activation function (typically ReLU). Apply another FC layer with a sigmoid activation function to obtain the recalibration weights as shown in Equation 3.

$$f_c = \sigma\,(W_2 . s_c + b_2) \quad (3)$$

Where f_c is the recalibration weight for channel c. W_2 and b_2 are the weights and bias of the second FC layer, respectively and σ is the sigmoid activation function.

Recalibration: Apply the recalibration weights to the original feature map by element-wise multiplication as shown in Equation 4.

$$y_{i,j,c} = f_c . x_{i,j,c} \quad (4)$$

Where y_(i,j,c) is the recalibrated feature map value at position (i, j) in channel c. This recalibrated feature map y now has enhanced channel-wise representations, with each channel's importance adjusted based on its relevance to the task. This SE block can be incorporated into a CNN architecture to improve its performance in various computer vision tasks.

Algorithm 1: Sequeeze and Excitation Pneumonia Prediction Block

Input: Dim = (H, W, C) # H stands for height, W for breadth, and C for channels.

x= Input radiograph/ feature maps

Notations: w = recalibration weights **Fig. 4.** VGG16 incorporating Squeeze and Excitation Block with “frozen” and trainable layers

r = intermediate reduction ratio r

y = rescaled feature maps

z = channel descriptor with dimensions (1, 1, C)

Fig. 4. VGG16 incorporating Squeeze and Excitation Block with "frozen" and trainable layers

FC= Fully connected Layer

Operation:

1. Input image tensors from VGG 16 block
2. Z(1,1,C)=Squeeze(x) # Spatial dimension condensation
3. Z = GlobalAveragePool(x)# Find channel descriptor
4. Return z
5. Excitation (z) #Models channel interdependencies
6. Fc1= FC (z, x/r) #Channel wise Recalibration
7. Fc1=relu(W1 *fc1)
8. Fc2 = FC(z, x)
9. W = σ(W2 * fc2) #Excitation Weights
10. Y = w * x # Scale and rescaling:
11. Output: Return y

The Squeeze-and-Excitation block takes a tensor as input as shown in Algorithm 1, applies fully connected layers with a reduction ratio, squeezes the operation global average pooling, and calculates the excitation weights using the sigmoid activation function. The excitation weights are then used to scale and rescale the input tensor.

The full deep network function has fully linked layers, convolutional layers, squeeze-and-excitation blocks, and an output layer. The architecture is made to take advantage of the SE mechanism to boost efficiency and provide better feature representation.

The Squeeze-and-Excitation (SE) technique enhances the representation strength of Convolutional Neural Networks by modeling channel interdependencies. It emphasizes channel-wise recalibration of weights, prioritizing educational channels and enabling adaptive feature recalibration. SE can be easily integrated into current best performing VGG16 architectures with minimal processing work, simplifying usage. Its inclusion improves performance in applications like semantic segmentation, object detection, and computer vision tasks. By modeling channel interdependencies, SE enhances discriminative information capture, accuracy, and generalization skills in pneumonia prediction.

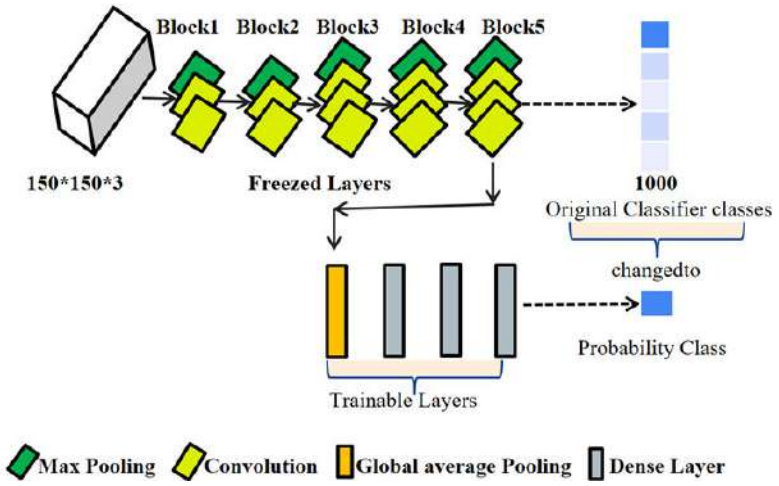

Fig. 4: VGG16 incorporating Squeeze and Excitation Block with "frozen" and trainable layers

4. RESULT AND DISCUSSION

The performance evaluation metrics like accuracy and loss during training and validation will be used for assessing proposed models. The severity of disease can be measured through opacification spread. The deep network parameters used for model training during preprocessing, augmentation, callback and fine tuning are as shown in Table 2.

Table 2: Proposed Squeeze and Excitation for VGG16 feature map calibration over network parameter fine tuning.

	Parameter	**Description**
Data Augmentation Parameters	Rescale	1/255
	Rotation Range	30
	Shear Range	10
	Zoom Range	0.2
	Horizontal Flip	True
	Width Shift Range	0.2
	Height Shift Range	0.2
	Fill_mode	nearest
Callback Parameters	Check logs	On epoch end
	Callback Condition	val_binary_accuracy>=0.98
	Action	Stop training
Training Parameters	steps_per_epoch	20
	epochs	100
	batch_size	16
	Image size	150*150
	Learning Rate schedule	Exponential Decay
Fine Tuning Parameters	Initial Learning Rate	1e-5
	Decay_steps	100000
	Decay_rate	0.96
	Optimizers.	RMSprop
	Loss	Binary crossentropy
	Metrics	Binary Accuracy

VGG16

VGG16 is a simple and detailed feature-based network for identifying pneumonia in chest X-Rays. Additional layers of batch normalisation are needed to increase the accuracy value in the detection of pneumonia. A connected dense layer for image classification are added on utilising two output neurons to divide the image into lung-infected or healthy categories. During training, it achieves 92.95% accuracy and 95% validation accuracy with a 0.16% loss. VGG16 model performance is as shown in Figure 4.

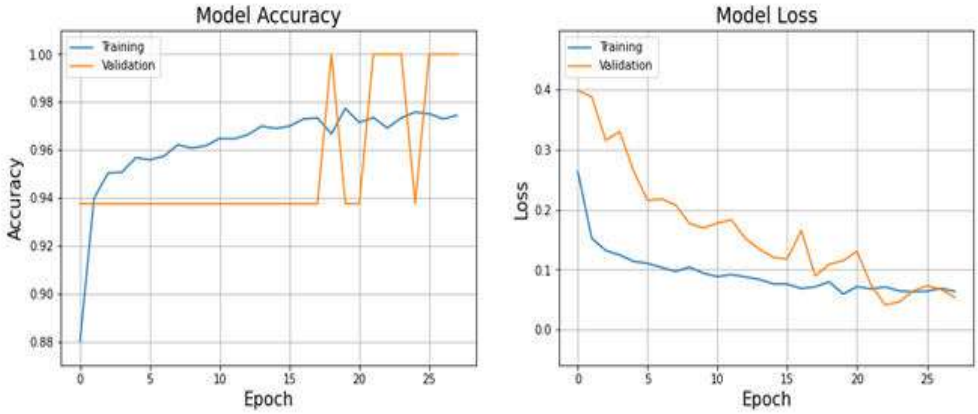

Fig. 4: Model Accuracy and Model Loss during training and validation using VGG 16 deep architecture for pneumonia disease detection using ImageNet.

Integrating Freeze VGG16 base model with Squeeze and Excitation Network

Squeeze and Excitation based disease categorization module output labels for a given input chest X-ray image include pneumonia or healthy. This module predicts chest X-ray classification and acts independently, calculating accuracy in percentage and loss Score to evaluate and measure the diagnostic performance using a single weighting function at the end, giving importance to individual features. This empowers the classification module to autonomously resolve the information significance from each image patch in thoracic image.

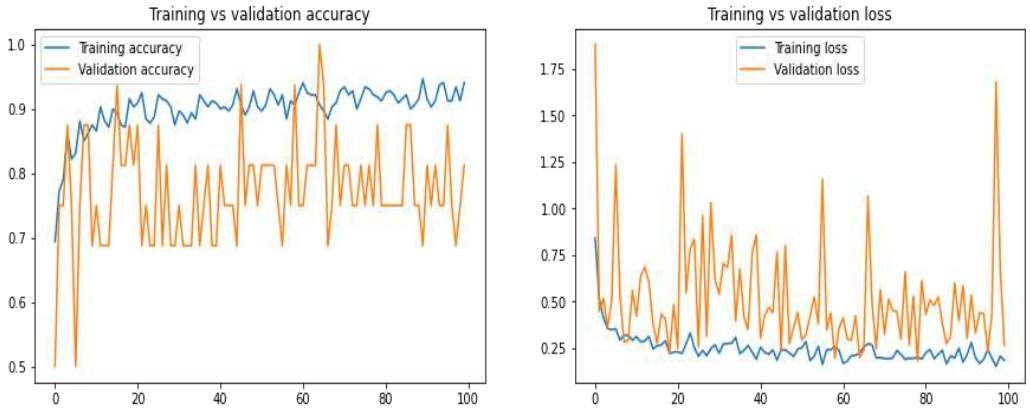

Fig. 5: VGG16 integration with SeNet over freeze feature extraction layers

Figure 5 shows that the performance of squeeze and excitation model built in integration with VGG16 with freezing the base feature extraction layers. Graph of epoch on x-axis verses accuracy score on y-axis clearly shows that the prediction performance for training the model was low in the initial epoch was increased slowly over increase in iterations. Similarly training loss of model was initially high slowly it went on decreasing as model was reaching convergence over increase in epochs. Validation performance of model is comparatively volatile but it also improved over higher epochs as shown in Figure 6.

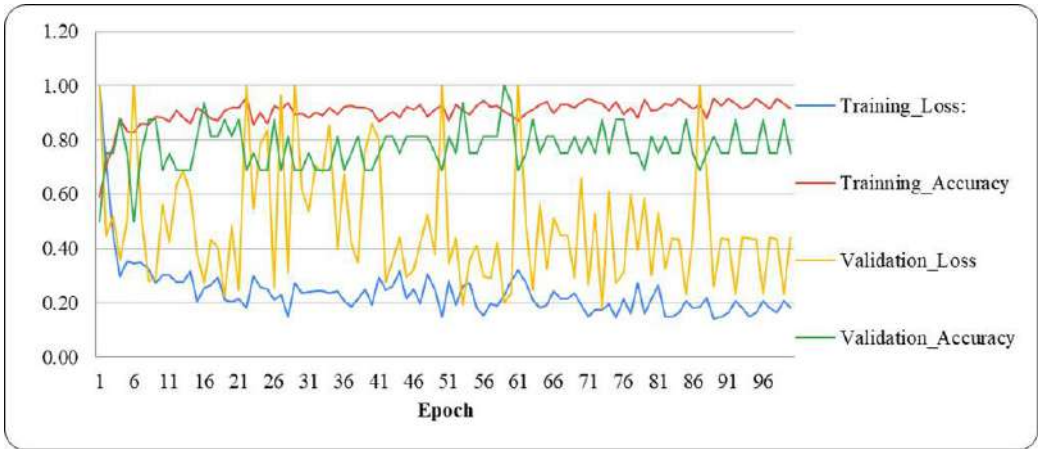

Fig. 6: Training and validation performance comparison of proposed transfer fusion model VGG16 integration with SeNet over freeze feature extraction layers

Improved VGG16 base model with adaptive Squeeze and Excitation Network

Performance of enhanced model having VGG16 pretrained architecture with unfreezing feature extraction base model loaded with additional Global average pooling and three dense layers of sizes 128, 64 with relu activation function and last one neuron at the output layer with sigmoid activation function. In order to avoid overfitting callback is set to validation performance at 98%, which indicates that model training will stop if validation accuracy reaches above set frequency. This updated model as shown in Figure 2 has higher evaluation performance compared to proposed base model as it has not retained the learned features from the original task but updated during training on the new task. Also additional layers help in layerwise feature building with more stable training performance and bit volatile validation evaluation performance as shown in Figure 7.

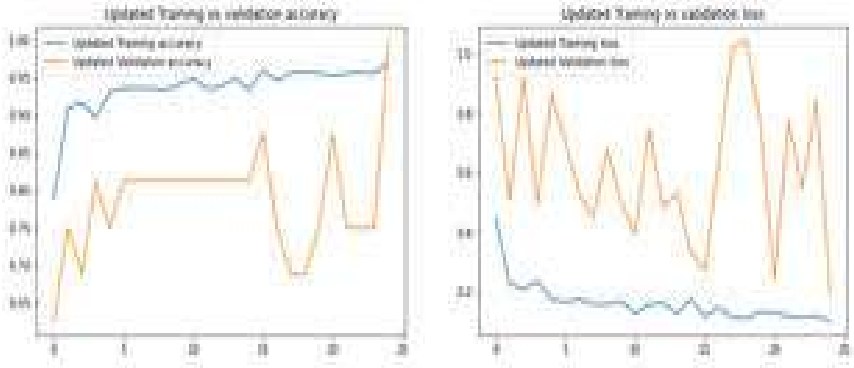

Fig. 7: VGG16 integration with SeNet over freeze feature extraction layers

Table 2 shows performance evaluation of proposed Squeeze and Excitation integration with VGG16 with state of art deep models such as EfficientNetB7, MobileNetV2, XceptionNet and VGG16. Table highlights that out of these transfer learning model VGG16 is the comparatively stable model which has better training as well as validation accuracy and needs moderate computational time. Hence VGG16 model is been selected as base model for feature extraction for further adaptive feature recalibration analysis. The proposed method gives better training accuracy but lower validation performance and model is updated with adaptive feature analysis layers which has global average pooling and additional dense layer at the end of the model which shows improvement in result with lesser training and validation loss. As more adaptive calibration, squeezing of layers and then integration with scaled feature maps brings additional burden results in more computational time. Proposed Updated SENet exhibits 96.69% Training accuracy and 09.89% Training Loss as compared to without freezing VGG16 weights Proposed considered SENet with VGG16 shows 94.16% Accuracy and 14.74 % Loss during training. In all

Proposed updatedVGG16 consolidation with SENet overperformes all existing techniques for pneumonia disease classification.

Figure 8 represents the intermediate layers extracted feature visualization. It clearly highlights that the feature extracted from block1 of first layer of convolutional block after pooling has very abstract representation of features. The preceeding layers are showing higher clear formation of lung region and feature detailing

Table 2: Performance evaluation of proposed deep model with state-of-art deep neural models

Deep Network	Train_ Acc	Train_ Loss	Val_ Loss	Val_ Acc	Time/ Epoch	Precision	Recall	F1-Score
EfficientNetB7	51.32	56.24	95.99	51.56	115.75	47.78	48.24	42.59
MobileNetV2	96.75	10.34	27.85	86.53	222.92	91.65	92.82	92.23
XceptionNet	93.89	27.09	45.58	87.50	735.57	85.51	93.85	89.49
VGG16	92.95	09.32	16.39	95.31	164.71	91.59	97.69	94.54
Proposed SENet	94.16	14.74	58.37	79.62	814.57	92.10	93.24	93.13
Proposed Updated SENet	**96.69**	**09.89**	**29.84**	**94.31**	**813.51**	**95.51**	**96.23**	**95.17**
Train_Acc → Training Accuracy Train_Loss → Training Loss Val_ Loss → Validation Loss Val_Acc → Validation Accuracy								

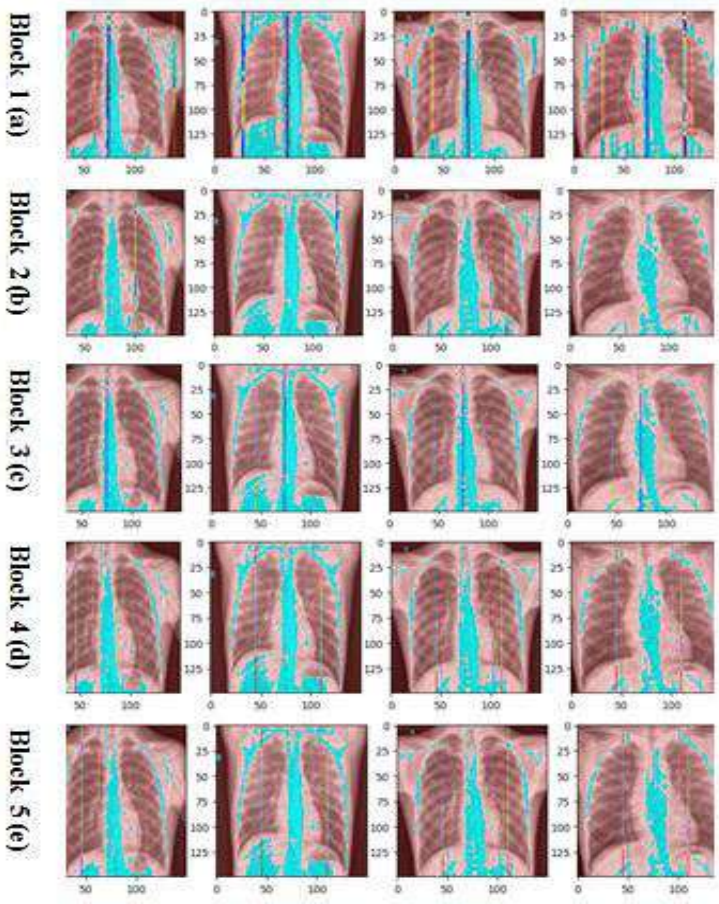

Fig. 8: Layer wise feature extraction visualization

5. CONCLUSION

Basic and improved squeeze and excitation block is integrated on the top of pretrained VGG16 model for calibration of extracted feature map by freezing and unfreezing base model learned weights to assign dynamic weights to feature maps contributing differently in pneumonia classification.. Squeeze and excitation network calibrates feature maps extracted from VGG16 model and assigns the appropriate weights to extracted feature maps based on its effectiveness in pneumonia disease prediction. It was observed that Squeeze and excitation block over unfreezing VGG16 base model with additional global average pooling and top 3 dense layers have a privilege to update the base model parameter weights shows higher performance accuracy compared to freeze parameter weights. Proposed updated SeNet model shows accuracy of 96.69% and loss of 09.89%.

As chest radiograph is an input to pneumonia detection model which is black and white in nature has no color channels information hence evaluation performance upgrades to limited range. Hence this research can be attractively extended to colorful image dataset in multiple research areas.

AUTHOR CONTRIBUTIONS

Kanchan Dabre: Methodology, Software, Writing- Original draft preparation.

Satishkumar L. Varma : Supervision, Conceptualization, Writing- Reviewing and Editing.

Pankaj B. Patil: Data curation, Visualization, Investigation and Validation..

Conflicts of interest

The authors declare no conflicts of interest.

6. REFERENCES

[1] Singh, S. and Tripathi, B. K. Pneumonia classification using quaternion deep learning. Multimedia Tools and Applications, 81(2), 1743–1764, 2022.

[2] Bodapati, J. D., and Rohith, V. N. (2022). ChxCapsNet: Deep capsule network with transfer learning for evaluating pneumonia in paediatric chest radiographs. Elsevier, Measurement: Journal of the International Measurement Confederation, 188, 2022.

[3] Bodapati, J., Devi, J., Vn, B. ·, · R., Dondeti, V., Bodapati, J. D., and Rohith, V. N. (2022). Ensemble of Deep Capsule Neural Networks: An Application to Pneumonia Prediction, arxiv, 2022.

[4] Islam, S. R., Maity, S. P., Ray, A. K., and Mandal, M. Deep learning on compressed sensing measurements in pneumonia detection. International Journal of Imaging Systems and Technology, 32 (1), 41–54, 2022.

[5] Dabre, Kanchan, Satishkumar L. Varma, and Pankaj B. Patil. "RAPID-Net: Reduced architecture for pneumonia in infants detection using deep convolutional framework using chest radiograph." Biomedical Signal Processing and Control 87 (2024): 105375.

[6] Stokes, K., Castaldo, R., Federici, C., Pagliara, S., Maccaro, A., Cappuccio, F., Fico, G., Salvatore, M., Franzese, M., and Pecchia, The use of artificial intelligence systems in diagnosis of pneumonia via signs and symptoms: A systematic review, Biomedical Signal Processing and Control (Vol. 72). Elsevier Ltd, 2022.

[7] Gare, G. R., Schoenling, A., Philip, V., Tran, H. v., Deboisblanc, B. P., Rodriguez, R. L., and Galeotti, J. M. (2021). Dense pixel-labeling for reverse-transfer and diagnostic learning on lung ultrasound for covid-19 and pneumonia detection, Proceedings - International Symposium on Biomedical Imaging, 1406–1410, April 2021.

[8] Tang, M. tian, Li, S., Liu, X., Huang, X., Zhang, D. ying, and Lei, M. xing. (2022). Early Detection of Pneumonia with the Help of Dementia in Geriatric Hip Fracture Patients. Orthopaedic Surgery, 14 (1), 129–138, 2021.

[9] Kosasih, K., Abeyratne, U. R., Swarnkar, V., and Triasih, R. (2015). Wavelet Augmented Cough Analysis for Rapid Childhood Pneumonia Diagnosis. IEEE Transactions on Biomedical Engineering, 62 (4), 1185–1194, 2015.

[10] Marini, T. J., Castaneda, B., Baran, and Kaproth-Joslin, K. A. (2019). Lung Ultrasound Volume Sweep Imaging for Pneumonia Detection in Rural Areas: Piloting Training in Rural Peru. Journal of Clinical Imaging Science, 9, 35, 2019.

[11] Ambroggio, L., Clohessy, C. and Shah, S. S. (2016). Lung Ultrasonography: A Viable Alternative to Chest Radiography in Children with Suspected Pneumonia, Journal of Pediatrics, 176 (7), 93-98, 2016.

[12] Liszewski, M. C., Görkem, S., Sodhi, K. S., and Lee, E. Y. (2017). Lung magnetic resonance imaging for pneumonia in children. Pediatric Radiology, 47 (11), 1420–1430, 2017.

[13] Saeed Ali Alzahrani, Majid Abdulatief, Al Salamah, Wedad Hussain, Al Madani, and Mahmoud A Elbarbary. Systematic review and meta - analysis for the use of ultrasound versus radiology in diagnosing pneumonia. Critical Ultrasound Journal, Springer, Open Access, pages 1-11, 2017.

[14] Yogendra Amatya, Jordan Rupp, Frances M Russell, Jason Saunders, Brian Bales, and Darlene R House. Diagnostic use of lung ultrasound compared to chest radiograph for suspected pneumonia in a resource-limited setting. International Journal of Emergency Medicine, Springer, Openaccess, pages 1-5, 2018.

[15] Sameer Antani. A review on lung boundary detection in chest X-rays. International Journal of Computer Assisted Radiology and Surgery, 2019.

[16] Vikash Chouhan, Sanjay Kumar Singh, Aditya Khamparia, Deepak Gupta, and Victor Hugo C De Albuquerque. applied sciences A Novel Transfer Learning Based Approach for Pneumonia Detection in Chest X-ray Images. Applied Sciences (Switzer-land) MDPI Journal, 10(2):1-17, 2020.

[17] Kermany Daniel S. Goldbaum Michael CaiWenjia Valentim Carolina C.S. and Liang. Identifying Medical Diagnoses and Treatable Diseases by Image-Based Deep Learning. Cell, Elsevier Inc., 172(5):1122-1131, 2018.

[18] Mingxia Liu Eds, International Workshop, and David Hutchison. Semantic-Aware Generative Adversarial Nets for Unsupervised Domain Adaptation in Chest X-Ray Segmentation. Machine Learning in Medical Imaging Springer Nature Switzerland AG, pages 143-151, 2018.

[19] Khalid El Asnaoui, Youness Chawki, and Ali Idri. Automated Methods for Detection and Classification Pneumonia based on X-Ray Images Using Deep Learning. arXiv, 2020.

[20] Tatiana Gabruseva, Dmytro Poplavskiy, and Alexandr Kalinin. Deep learning for automatic pneumonia detection. IEEE Computer Society Conference on Computer Vision and Pattern Recognition Workshops, June:1436-1443, 2020.

[21] Bram Van Ginneken, M Bart, Haar Romeny, and Max A Viergever. Computer-Aided Diagnosis in Chest Radiography: A Survey. IEEE Transaction on Medical Imaging, 20(12):1228-1241, December 2001.

[22] Yu Gordienko, Peng Gang, Jiang Hui, Wei Zeng, Yu Kochura, and O Alienin. Deep Learning with Lung Segmentation and Bone Shadow Exclusion Techniques for Chest X-Ray Analysis of Lung Cancer. ICCSEEA, Springer International Publishing AG, part of Springer Nature 2019, 754:638-647, 2019.

[23] Xianghong Gu, Liyan Pan, Huiying Liang, and Ran Yang. Classification of Bacterial and Viral Childhood Pneumonia Using Deep Learning in Chest Radiography. ACM, ICMIP 2018, pages 88-93, 2018.

[24] John R Zech Id, Marcus A Badgeley Id, Manway Liu Id, Anthony B Costa Id, J Titano, Eric Karl, and Oermann Id. Variable generalization performance of a deep learning model to detect pneumonia in chest

radiographs: A cross-sectional study. OPEN ACCESS, J. PLOS Medicine, pages 1-17, 2018.

[25] Amit Kumar Jaiswal, Prayag Tiwari, Sachin Kumar, Deepak Gupta, Ashish Khanna, and Joel J.P.C. Rodrigues. Identifying pneumonia in chest X-rays: A deep learning approach. Measurement: Journal of the International Measurement Confederation, 145:511-518, 2019.

[26] Wasif Khan, Nazar Zaki, and Luqman Ali. Intelligent Pneumonia Identification from Chest X-Rays: A Systematic Literature Review. medRxiv preprint, pages 1-13, 2020.

[27] Septy Aminatul Khoiriyah. Convolutional Neural Network for Automatic Pneumonia Detection in Chest Radiography. IEEE, pages 476-480, 2020.

[28] Mahreen Kiran, Imran Ahmed, Nazish Khan, and Alavalapati Goutham Reddy. Chest X-ray segmentation using Sauvola thresholding and Gaussian derivatives responses. Journal of Ambient Intelligence and Humanized Computing, 10(10):4179-4195, 2019.

[29] Bing N A N Li, Senior Member, Jing Qin, Rong Wang, Meng Wang, and Xuelong Li. Selective Level Set Segmentation Using Fuzzy Region Competition. IEEE Access, 4:4777-4788, 2016.

[30] Yuanyuan Li, Zhenyan Zhang, Cong Dai, Qiang Dong, and Samireh Badrigilan. Accuracy of deep learning for automated detection of pneumonia using chest X-Ray images: A systematic review and meta-analysis. Computers in Biology and Medicine, 123(May):103898, 2020.

[31] Gaobo Liang and Lixin Zheng. A transfer learning method with deep residual network for pediatric pneumonia diagnosis. Computer Methods and Programs in Biomedicine, Elsevier, 187:1-9, 2020.

[32] Tanvir Mahmud, Md Awsafur Rahman, and Shaikh Anowarul Fattah. CovXNet: A multi-dilation convolutional neural network for automatic COVID-19 and other pneumonia detection from chest X-ray images with transferable multi-receptive feature optimization. Computers in Biology and Medicine, 122:103869, May 2020.

[33] Ansh Mittal, Deepika Kumar, Mamta Mittal, Tanzila Saba, Ibrahim Abunadi, Amjad Rehman, and Sudipta Roy. Detecting Pneumonia using Convolutions and Dynamic Capsule Routing for Chest X-ray Images. MDPI, sensors Article, pages 1-30, 2020.

[34] Faizan Munawar, Shoaib Azmat, Talha Iqbal, Christer Gronlund, and Hazrat Ali. Segmentation of Lungs in Chest X-Ray Image Using Generative Adversarial Networks. IEEE Access, Open Access Journal, 8:153535-153545, 2020.

[35] Alexey A. Novikov, Dimitrios Lenis, David Major, Jiri Hladuvka, Maria Wimmer, and Katja Buhler. Fully Convolutional Architectures for Multiclass Segmentation in Chest Radiographs. IEEE Transactions on Medical Imaging, 37(8):1865-1876, 2018.

[36] Prakhar Gupta Prateek Chhikara, Prabhjot Singh andpreet Bhatia. Deep Convolutional Neural Network with Transfer Learning for Detecting Pneumonia on Chest X-Rays. Advances in Intelligent Systems and Computing 1064 Advances in Bioinformatics, Multimedia, and Electronics Circuits and Signals, pages 155-168,2019.

[37] Chunli Qin, Demin Yao, Yonghong Shi, and Zhijian Song. Computer-aided detection in chest radiography based on artificial intelligence: A survey. Springer Journal on BioMedical Engineering Online, 17(1):1-23, 2018.

[38] Tawsifur Rahman, Muhammad E H Chowdhury, and Amith Khandakar. Applied sciences Transfer Learning with Deep Convolutional Neural Network (CNN) for Pneumonia Detection Using. MDPI, J. app Sci., 3233:1-17, 2020.

[39] Moritz Schwyzer, Katharina Martini, Stephan Skawran, Michael Messerli, and Thomas Frauenfelder. Pneumonia Detection in Chest X-Ray Dose-Equivalent CT: Impact of Dose Reduction on Detectability by Artificial Intelligence. Elsevier, Academic Radiology, pages 1-5, 2020.

[40] Ilyas Sirazitdinov, Maksym Kholiavchenko, and Tamerlan Mustafaev. Deep neural network ensemble for pneumonia localization from a large-scale chest x-ray database. Elsevier, J.Computers and Electrical Engineering, 78:388-399, 2019.

[41] Okeke Stephen, Mangal Sain, Uchenna Joseph Maduh, and Do Un Jeong. An Efficient Deep Learning Approach to Pneumonia Classification in Healthcare. Journal of Healthcare Engineering, pages 1-7, 2019.

[42] M. Togacar, B. Ergen, Z. Comert, and F. Ozyurt. A Deep Feature Learning Model for Pneumonia Detection Applying a Combination of mRMR Feature Selection and Machine Learning Models. Irbm, 41(4):212-222, 2020.

[43] Andrea Valsecchi and Oscar Cordo. Deep architectures for high-resolution multiorgan chest X-ray image segmentation. Springer, Nature,Neural Computing and Applications, 2, 2019.

[44] Tej Bahadur Chandra Verma and Kesari. Pneumonia Detection on Chest X-Ray using Machine Learning Paradigm, Advances in Intelligent Systems and Computing 1022, volume 1. 3rd International Conference on Computer Vision and Image Processing, 2018.

[45] Jianpeng Zhang, Yutong Xie, Guansong Pang, Zhibin Liao, Johan Verjans, Wenxing Li, and Zongji Sun. Viral Pneumonia Screening on Chest X-rays Using Confidence Aware Anomaly Detection. IEEE Transaction on Medical Imaging, 23(12), November 2020.

[46] T. J. Marini et al., "Lung Ultrasound Volume Sweep Imaging for Pneumonia Detection in Rural Areas: Piloting Training in Rural Peru," J. Clin. Imaging Sci., vol. 9, no. xx, p. 35, 2019.

[47] L. Ambroggio et al., "Lung Ultrasonography: A Viable Alternative to Chest Radiography in Children with Suspected Pneumonia?," J. Pediatr., vol. 176, pp. 93-98.e7, 2016.

[48] A. Sharma and D. Raju, "Detection of Pneumonia clouds in Chest X-ray using Image processing approach" IEEE Conf, 978-1-5386-1747-2/17, vol. 17, pp. 0–3, 2017.

[49]]P. Konietzke et al., "The value of chest magnetic resonance imaging compared to chest radiographs with and without additional lung ultrasound in children with complicated pneumonia," PLoS One, vol. 15, no. 3, pp. 7–13, 2020.

[50] M. C. Liszewski, S. Görkem, K. S. Sodhi, and E. Y. Lee, "Lung magnetic resonance imaging for pneumonia in children," Pediatr. Radiol., vol. 47, no. 11, pp. 1420–1430, 2017.

[51] Kermany Daniel, Zhang Kang, Goldbaum Michael, "Labeled Optical Coherence Tomography (OCT) and Chest X-Ray Images for Classification", Mendeley Data, V2, doi: 10.17632/rscbjbr9sj.2, 2018.

[52] Z. Ren, Y. Zhang, and S. Wang, "LCDAE: Data Augmented Ensemble Framework for Lung Cancer Classification," Technol. Cancer Res. Treat., vol. 21, 2022.

[53] R. E. Al Mamlook, S. Chen, and H. F. Bzizi, "Investigation of the performance of Machine Learning Classifiers for Pneumonia Detection in Chest X-ray Images," IEEE Int. Conf. Electro Inf. Technol., vol. 2020-July, pp. 98–104, 2020.

[54] F. Wahid, S. Azhar, S. Ali, M. S. Zia, F. Abdulaziz Almisned, and A. Gumaei, "Pneumonia Detection in Chest X-Ray Images Using Enhanced Restricted Boltzmann Machine," J. Healthc. Eng., vol. 2022.

[55] Alharbi AH, Hosni Mahmoud HA. Pneumonia transfer learning deep learning model from segmented X-rays. InHealthcare 2022 May 26 (Vol. 10, No. 6, p. 987). MDPI.

[56] Gabruseva T, Poplavskiy D, Kalinin A. Deep learning for automatic pneumonia detection. InProceedings of the IEEE/CVF conference on computer vision and pattern recognition workshops 2020 (pp. 350-351).

[57] Ayan E, Karabulut B, Ünver HM. Diagnosis of pediatric pneumonia with ensemble of deep convolutional neural networks in chest x-ray images. Arabian Journal for Science and Engineering. 2022 Feb 1:1-7.